Rate of coastal temperature rise adjacent to a warming western boundary current is non-uniform with latitude

Neil Malan [1,2]**, Moninya Roughan**[1,2]**, Colette Kerry** [1,2]

[1]School of Mathematics and Statistics, UNSW Sydney, NSW, Australia
[2]Centre for Marine Science and Innovation, UNSW Sydney, NSW, Australia

Key Points:

- Temperature trends on a western boundary shelf are 2x greater poleward of the separation point than equatorward of the separation point.
- Equatorward of the separation point, mean kinetic energy increases, while poleward (downstream) eddy kinetic energy increases.
- This latitudinal difference in warming is driven by increased eddy driven heat advection onto the shelf downstream of the separation point.

Corresponding author: Neil Malan, `neilcmalan@gmail.com`

Abstract

Western boundary currents (WBCs) have intensified and become more eddying in recent decades due to the spin-up of the ocean gyres, resulting in warmer open ocean temperatures. However, relatively little is known of how WBC intensification will affect temperatures in adjacent continental shelf waters where societal impact is greatest. We use the well-observed East Australian Current (EAC) to investigate WBC warming impacts on shelf waters and show that temperature increases are non-uniform in shelf waters along the latitudinal extent of the EAC. Shelf waters poleward of 32°S, are warming more than twice as fast as those equatorward of 32°S. We show that non-uniform shelf temperature trends are driven by an increase in lateral heat advection poleward of the WBC separation, along Australia's most populous coastline. The large scale nature of the process indicates that this is applicable to WBCs broadly, with far-reaching biological implications.

Plain Language Summary

As the circulation in ocean basins intensifies, it causes changes in the currents on their western boundaries which carries heat towards the poles. While we know that this causes warming in the open ocean, knowledge of how these changes affect coastal and shelf regions is limited. Here we use a suite of different observations and an ocean model to show that, off the coast of southeastern Australia, the coastal ocean is warming two or three times faster in areas poleward of where the East Australian Current separates from the coast than where the East Australia Current remains close to the coast. This is due to the shelf waters poleward of where the current separates from the coast receiving an increase in the amount of warm water being pushed onto them as the southern outflow of the East Australia Current becomes more turbulent and eddying. This warming is driven by large scale changes in wind patterns, and so is likely to be common to other similar current systems. As coastal ecosystems are the most productive, we expect this non-uniform warming to have a widespread biological impact.

1 Introduction

1.1 Global gyre spin-up and impacts

Globally, oceanic kinetic energy has been increasing since the early 1990's (S. Hu et al., 2020), and the subtropical gyres, which act via their western boundary currents as the major driver of poleward heat, have intensified, extended poleward, (Yang et al., 2015, 2020) and warmed (Wu et al., 2012). However, western boundary currents are highly non-linear systems, and their response to the spin up of the subtropical gyres is not completely understood (Imawaki et al., 2013; Beal & Elipot, 2016; Hutchinson et al., 2018). Furthermore, understanding changes in the interaction between western boundary currents and shelf waters is challenging, due to fine temporal and spatial scales and the energetic nature of the interactions. Thus, while there are several studies on warming within western boundary current extensions in the blue ocean (Wu et al., 2012; Williams, 2012; Chen et al., 2014), there is little understanding of how continental shelf waters inshore of western boundary currents are responding to subtropical gyre intensification. This is partly due to a lack of suitable long-term observations (Shearman & Lentz, 2010) and the uncertainty in using satellite and reanalyses products close to the coast in areas of strong velocity and temperature gradients.

1.2 South Pacific gyre spin up and impacts

In response to the intensification of the south pacific gyre circulation, the East Australian Current (EAC) extension region has been warming at two to three times the global average since the early 1990s (D. Hu et al., 2015; Qu et al., 2019). However, with most

attention on changes in the separation latitude and the nature of eddies in the EAC extension region (Cetina-Heredia et al., 2014; Oliver & Holbrook, 2014; Rykova & Oke, 2015), there has been little investigation into whether the effect of the spin up on the EAC is homogeneous. Of the many studies that have investigated a system-wide temperature response to climate change, they mostly have global to basin-scale focus (Wu et al., 2012; Oliver & Holbrook, 2014; Bowen et al., 2017; Duran et al., 2020; Bull et al., 2020) with little investigation into latitudinal dependence. A knowledge of this latitudinal dependence is particularly important considering the societal benefit derived from coastal and shelf waters particularly fisheries (Suthers et al., 2011), the large range of dynamical regimes, and the tropicalisation of ecosystems (Vergés et al., 2014; Messer et al., 2020) occurring in WBCs, e.g in the EAC between 26°S and 40°S.

1.3 EAC shelf temperature trends

Previous studies of temperature trends in the EAC cover a very limited latitudinal range. Thompson et al. (2009), using historical in-situ surface data found a coastal temperature trend of 0.7°C per century at Port Hacking (34°S) and 2°C per century at Maria Island (42°S). The warming trend at Maria Island has been attributed to changes to basin-scale wind forcing, and thus intensification of the EAC (Hill et al., 2008). Later work using coupled climate models suggest the much of this intensification may in fact be driven by regional changes in wind stress curl (Bull et al., 2020). Thus, there appears to be a link between the intensification of the subtropical gyre circulation and increasing temperature trends on the continental shelf. However, this is based on one observational site at 42°S (Hill et al., 2008; Shears & Bowen, 2017), at the southern most extent of the EAC extension far from the influence of the EAC jet itself. Moreover, there is little knowledge of the response of the EAC shelf system along its latitudinal range (greater than 2000 km) to the intensification of the EAC.
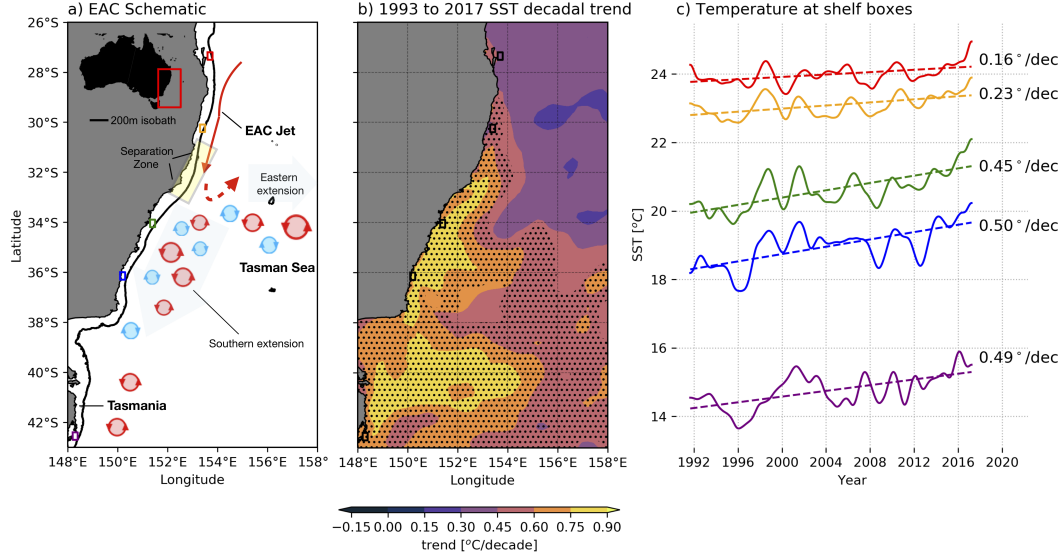
1.4 Approach

Previous work looking at changes in coastal latitudinal temperature gradients (Baumann & Doherty, 2013) uses gridded temperature data which is too coarse to resolve western boundary shelf systems, where length scales are 10-40km (Schaeffer et al., 2016). In the East Australian Current (EAC), the Integrated Marine Observing System has maintained an array of shelf moorings since 2008, along the length of the EAC, from 27°S to 42°S. Here we use this long-term of in-situ temperature observations, long-term satellite derived datasets and a multi-decadal regional ocean model simulation to investigate the nature of change in the EAC system from 1993 to 2020. We focus on how large scale changes in the dynamics affect temperatures in continental shelf waters between (26°S) and (42°S). Whilst no single dataset can fully represent the state of this narrow (< 50km) stretch of shelf water between the dynamic western boundary current and the coast, the integration of these different methods allows a robust view of changes in the system.

2 Data and Methods

2.1 Satellite sea surface temperature

Satellite derived foundation sea surface temperatures (SST) are obtained from the Group for High Resolution Sea Surface Temperature (GHRSST) Level 4 SST analysis produced at the Canadian Meteorological Center. This dataset merges infrared satellite SST at varying points in the timeseries from the ATSR series of radiometers from ERS-1, ERS-2 and Envisat, AVHRR from NOAA-16,17,18,19 and METOP-A, and microwave data from TMI, AMSR-E and Windsat in conjunction with in-situ observations of SST from ships and drifting buoys. This product performs well when compared to other long-term gridded SST analyses (Fiedler et al., 2019), while still retaining sufficient res-

olution for use on the shelf. Temperature timeseries for shelf waters are extracted by averaging satellite SST over a 0.2° x 0.3° box around the shelf mooring locations shown in Table 1. SST trends are calculated from a linear regression of the annual means (from 1993-2017) after the climatological season cycle was removed. Significance is calculated at a 95% confidence interval using the Wald Test with t-distribution of the test statistic.

Figure 1. a) Schematic of East Australian Current system, with mooring site shelf boxes marked in colour, b) Decadal trend of satellite derived SST where stippling indicates significance at 95% confidence interval, c) Timeseries of 2 year low-pass filtered satellite derived SST and decadal linear trend at shelf mooring locations as shown by the coloured boxes in a) and b): red 27°S, orange 30°S, green 34°S, blue 36°S and purple 42°S.

2.2 In situ temperature observations

To evaluate whether the trends derived from satellite SST are an appropriate representation of changes in temperatures along the shelf, we compare them with near-surface in-situ temperature observations from shelf moorings. Data are obtained from the Integrated Marine Observing System (IMOS) Australian National Mooring Network who maintain moorings at 27°S, 30°S, 34°S, 36°S and 42°S. The moored temperature data records are at least a decade long, with the earliest record used here starting in 2008. Temporal sampling is 5 min to hourly since commencement, with 'near-surface' records ranging 12-23m below the surface in water depths of 63-140m (see Table 1). Hence they are extremely useful for validating the long-term shelf temperature trends observed by satellite over a large latitudinal range ($\sim$ 1600km).

2.3 Eddy and mean kinetic energy

Sea surface height observations and derived geostrophic velocities (u and v) were obtained from the satellite altimetry product distributed by IMOS (accessed at portal.aodn.org.au). This product merges satellite altimetry with sea level elevation measurements from coastal tide gauges (Deng et al., 2011) with a spatial resolution of 0.2°. The eddy and mean kinetic energy (EKE and MKE, shown in Fig. 2) were calculated for the period 1993 to 2017. EKE is defined as $(u'^2 + v'^2)/2$, where $u' = u - \bar{u}$ and $v' = v - \bar{v}$; $\bar{u}$ and $\bar{v}$ being

the annual mean for each individual year. MKE is defined as $(\bar{u}^2 + \bar{v}^2)/2$. The time-series for EKE are extracted from boxes 0.5° x 0.5°, which are larger than for SST, due to the lower resolution of the altimetry. Trends and statistical significance are calculated as detailed for SST above.

Table 1. Metadata for the in situ temperature observations obtained at the shelf mooring sites along southeastern Australia (Latitude (°S), mooring depth (m) and sensor depth (m), start date through to present, percentage data coverage for each moored temperature record). Also shown are the correlations between the moored temperature data and satellite SST, the temperature trend at each location, where trend is the decadal trend from the start of the time series until the end of 2019, and the 10m depth temperature trend from EAC-ROMS for the period 1994-2016.

Latitude (°S)	Mooring depth [m]	Sensor depth [m]	Start date	Data coverage [%]	Corr. with SST	Trend start-2019 [°C/decade]	EAC-ROMS trend [°C/decade]
27.34	63	20	2010-12-13	92	0.90	0.1	0.06
30.27	100	12	2010-02-20	97	0.92	0.5	-0.04
34.00	140	23	2008-06-25	83	0.90	0.9	0.46
36.22	120	19	2011-03-29	82	0.93	1.6	0.61
42.60	90	20	2008-04-08	95	0.98	1.4	N/A

2.4 Heat Budget

A regional hydrodynamic model of the EAC system (EAC-ROMS) (Kerry & Roughan, 2020a, 2020b) is used to further our understanding of the drivers of temperature on the shelf adjacent to the EAC. The model uses the Regional Ocean Modelling System (ROMS) and the configuration has been used in previous studies of the EAC system (Kerry et al., 2016; Rocha et al., 2019; Kerry & Roughan, 2020a; Kerry et al., 2020; Schilling et al., 2020; Phillips et al., 2020). The domain extends from 25.3°S to to 38.5°S, and from the coast to ∼1000km offshore. The grid is rotated 20° clockwise so as to be aligned with the shelf edge. Spatial resolution is 5km in the along-shelf direction and 2.5km in the cross-shelf direction, giving a good representation of the hydrodynamics of the shelf waters inshore of the EAC. The model runs from 1994 to 2016. Full details of the model set up and validation can be found in Kerry et al. (2016); Kerry and Roughan (2020a), for validation of temperature trends, please see supplementary material. EAC-ROMS provides a dynamically consistent high resolution framework with which to assess the varied contributions of lateral advection of heat and surface heat flux to temperature changes in shelf waters.

We investigate the heat budget in EAC-ROMS to assess changes in both atmospheric forcing and oceanic heat advection in shelf waters following previous studies (Zaba et al., 2020; Tamsitt et al., 2016; Colas et al., 2012). The depth-averaged shelf heat budget can be simplified to:

$$\frac{dT}{dt} = ADV + Qs \tag{1}$$

Where the temperature tendency $\frac{dT}{dt}$ (from here on referred to as TEND) is a function of the lateral heat transport (ADV - from advection plus a small contribution from horizontal diffusion and mixing) and the flux of heat between ocean and atmosphere (Qs, referred to as SURF). Use of the online diagnostic terms in the model enables the budget to close, as by design the model satisfies the heat conservation equations. Temperature tendency can be represented for volume V as the spatially and depth integrated

164   rate of change of each term in a box as:

165
$$\underbrace{\iiint_V \frac{dT}{dt}}_{\text{TEND}} = \underbrace{\iiint_V (\boldsymbol{u} \cdot \nabla T)dV + T_{diff}}_{\text{ADV}} + \underbrace{\iint_A Qs}_{\text{SURF}} \tag{2}$$

166   These terms are calculated at each of the four shelf sites in a 0.2° x 0.3° box co-located
167   with the mooring and satellite data.

3 Results

3.1 Sea surface temperature trends

170   Spatial maps of satellite SST trends in the Tasman Sea/EAC region (Fig. 1b) show
171   significant temperature increases poleward of 30°S since 1991. These are initially con-
172   fined along the coast, but poleward of 34°S temperature increases extend offshore into
173   the Tasman Sea. The strongest warming, approaching 1°C/decade is along the coast be-
174   tween 32°S and 38°S, and also at 40°S to the east of Tasmania (Fig. 1b). To explore trends
175   over the continental shelf, we examine SST timeseries extracted from 0.2° x 0.3° boxes
176   co-located with shelf mooring sites (coloured boxes marked on Fig 1a). Here we see the
177   rate of warming increases with latitude. At 27°S and 30°S, the linear SST trends are 0.16°C/decade
178   and 0.23°C/decade respectively, between 1991 and 2017. Downstream of the mean EAC
179   separation point, at 34°S, 36°S and 42°S, SST has warmed at approximately 0.5°C/decade
180   between 1991 and 2017 (Fig. 1c).

181   The comprehensive shelf mooring array off southeast Australia allows a similar lat-
182   itudinal analysis to be performed using in-situ shelf temperature observations. Despite
183   the relatively shorter timeseries, gaps in the record, and assorted start dates and mea-
184   surement depths of the shelf mooring sites (Table 1), correlations are high. Correlation
185   coefficients between daily satellite SSTs (averaged over a 0.2° x 0.3° box around the moor-
186   ing location) and in-situ moored observations are 0.9 or greater at all sites. As the moored
187   observations begin more recently than the other timeseries, they show stronger trends,
188   due to warming accelerating over time.

189   Temperature trends calculated from the moored temperature observations follow
190   the same broad pattern as the satellite SSTs. Poleward sites (34°S, 36°S and 42°S) are
191   warming at approximately two to three times the rate of the equatorward sites at 27°S
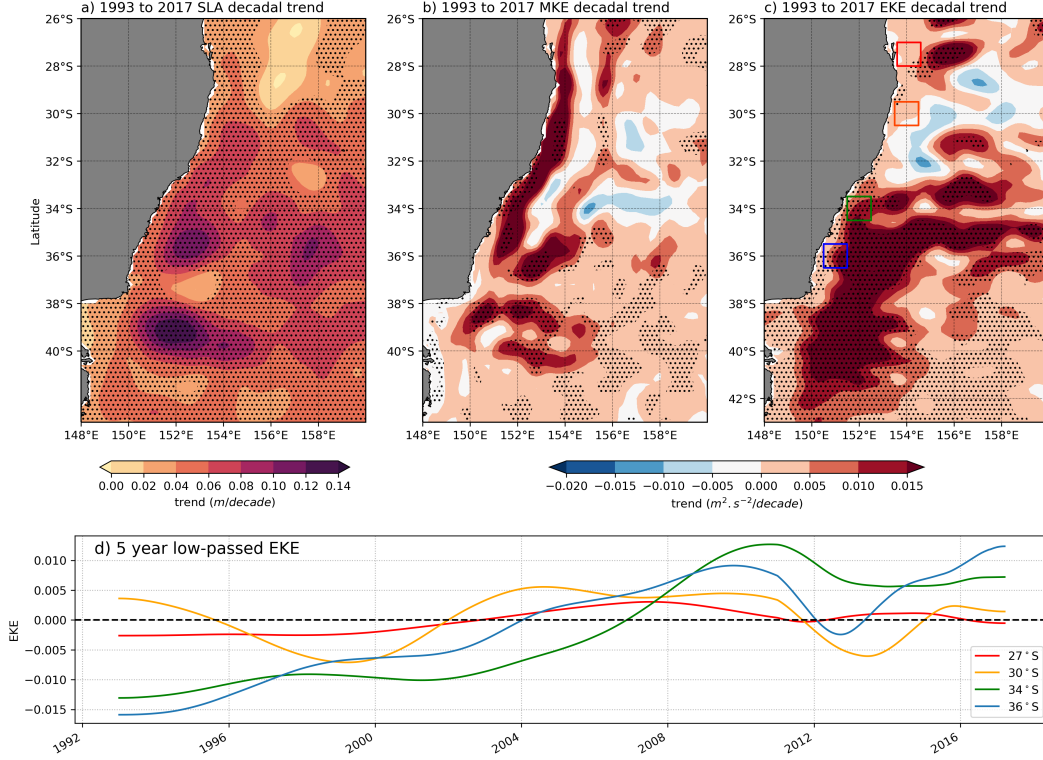192   and 30°S.

193   As with both the satellite SST and moored in-situ temperatures, depth-averaged
194   shelf temperature trends from 1994-2016 from the EAC-ROMS model follow the same
195   pattern where sites poleward of the EAC separation point have warmed more than twice
196   as fast as those equatorward of separation. At 27°S the depth averaged warming rate
197   is 0.07°/decade, at 30°S 0.12°/decade, at 34°S 0.37°/decade and at 36°S 0.29°/decade.
198   EAC-ROMS trends of temperature taken at 10m depth are shown in Table 1 for com-
199   parison with satellite SST.

3.2 Trends in kinetic energy

201   With previous work having linked warming in the Tasman Sea to an intensifica-
202   tion of the EAC system (Hill et al., 2008), we now investigate changes in the mesoscale
203   circulation as a possible driver of shelf water temperature change over 25 years from 1993-
204   2017. There are significant increases in sea level anomaly (SLA) throughout most of the
205   domain (Fig 2a), with the largest increasing trends occurring in roughly circular struc-
206   tures in the western Tasman Sea at 35°S and 39°S.

207   Decomposing these sea level changes into MKE and EKE trends is revealing. EKE
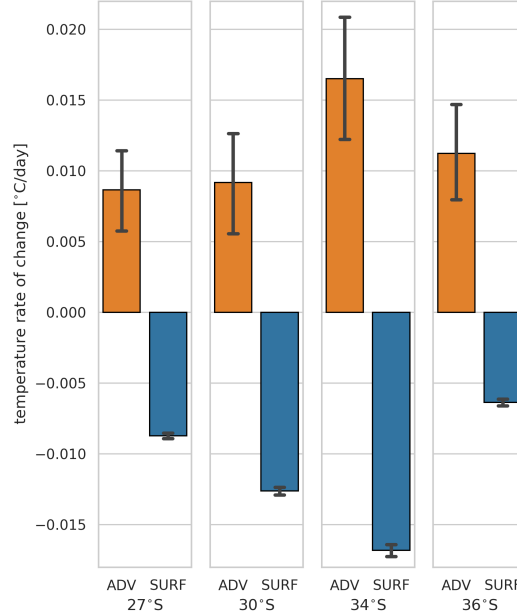208   has increased significantly (significance marked by cross hatching) downstream of the

Figure 2. Decadal trend (from 1993 to 2017) in (a) Sea level Anomaly, (b) Mean kinetic energy, c) Eddy kinetic energy, with anomalies extracted over coloured boxes for d) timeseries of eddy kinetic energy anomalies (5 year Hanning filter, seasonal cycle removed).

209 typical EAC separation point at 32°S. There is a small decrease in EKE at the offshore
210 edge of the main EAC jet, but it is not significant (Fig 2b). There are increases in MKE
211 along the full length of the EAC between 28°S and 36°S, which points to an increase in
212 both the strength of the EAC jet itself, and EAC separation occurring progressively fur-
213 ther poleward (in agreement with Cetina-Heredia et al. (2014)). In EAC-ROMS we see
214 broad agreement with the satellite observations. The model shows a reduction in EKE
215 in the EAC eastern extension and an increase in EKE in the EAC southern extension,
216 south of separation (Fig. S2).

217   Thus, while the main EAC jet is intensifying between 28°S and 34°S, the warm-
218 ing trends over the adjacent shelf are low (0.16-0.23°/decade, Fig. 1c, Table 1). The re-
219 gion where shelf temperatures are warming the fastest (0.5 °/decade), i.e. south of 34°S,
220 is where there are significant increases in EKE both offshore, and over the shelf. This
221 is consistent with Cetina-Heredia et al. (2014) who showed an increase in eddy driven
222 poleward transport in the EAC system since 2010 and in line with modelled projections
223 for an increase in the strength of the EAC's southern extension (Oliver & Holbrook, 2014).

224   While the case for a stronger, more eddying EAC extension driving warming in the
225 Tasman Sea broadly is relatively well established, the drivers of shelf temperature trends
226 appear to be more nuanced. On the shelf, shallow bathymetry can limit the influence
227 of large mesoscale eddies, and upwelling dynamics are complex (Roughan & Middleton,
228 2002; Schaeffer et al., 2013). It is possible that the strong vorticity gradient associated
229 with the EAC jet equatorward of separation is reducing the impact of the intensifica-
230 tion of the EAC system on shelf temperatures between 28°S and 30°S as these shelf wa-

ter are already strongly influenced by the EAC (Archer et al., 2017). Conversely, pole-
ward of separation the increase in eddy activity could result in increased cross-shelf trans-
port of warm offshore water onto the shelf (Malan et al., 2020; Cetina-Heredia et al., 2019),
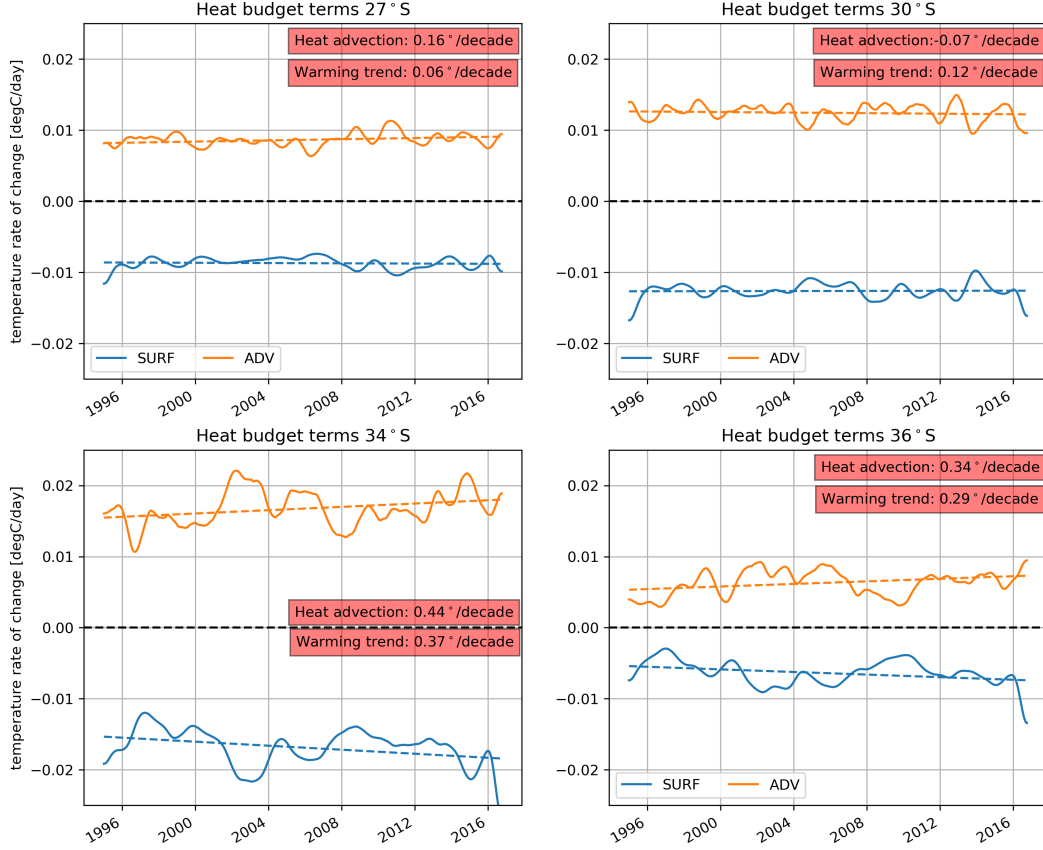thus driving the faster warming rate at 34°S and 36°S.

Figure 3.   Time and area-averaged terms in the depth averaged heat budget (Advection and
Surface flux) calculated from EAC-ROMS output over the shelf at 27°S, 30°S, 34°S and 36°S,
period 1994-2016. Error bars represent 95% confidence intervals.

3.3 Linkages between shelf temperature and kinetic energy trends

In order to understand the drivers of the observed warming gradient along the south-
east Australian coastline, heat budget terms from the EAC-ROMS simulation are ex-
amined at each shelf box over the 22 year period. At 27°S, 30°S, 34°S and 36°S, the depth-
averaged terms are calculated over a 0.2° x 0.3° box, co-located with the mooring and
satellite SST timeseries (Fig 1b). As expected in a western boundary current system,
at all sites advection warms the water column (positive dT/dt), whilst surface heat fluxes
from ocean to atmosphere cool the water column (negative dT/dt). The mean advec-
tive heat flux is smallest at 27°S, where the EAC is at its most stable (standard error
is also smallest). Advection driven heat fluxes increase poleward, nearly doubling at 34°S,
in the EAC separation zone, before decreasing at 36°S. This advective heating is coun-
tered by the surface heat flux from ocean to atmosphere. It should be noted that the ad-
vective heat flux in our shelf boxes has a high level of variability at all latitudes (great-
est at 34°S) indicative of the variable nature of the EAC, as shown by the large 95% con-
fidence interval error bars in Fig. 3, while surface heat fluxes are less variable.

Investigating the warming trend over the two decades shows that trends in the tem-
perature rate of change driven by advection are weak at 27°S and 30°S (upstream of the
EAC separation), but increase downstream of the EAC separation to 0.44°/decade at
34°S and 0.34°/decade at 36°S (Fig. 4). Thus it would appear from both satellite ob-
servations and the model that an intensification of the mean flow of the EAC does not
result in rapid warming of shelf waters, while an increase in eddy activity does. At the
event scale, this increase in the advection of warm EAC water onto the shelf via an in-

Figure 4. Timeseries of mean of daily area-averaged heat budget terms from EAC-ROMS for shelf boxes at 27°S, 30°S, 34°S and 36°S. Decadal trends for depth-averaged temperature and heat advection are shown for each box.

tensification of the eddying EAC southern extension has also been identified as a possible driver of marine heat-wave events (Oliver et al., 2017; Schaeffer & Roughan, 2017).

4 Discussion and Conclusions

As the EAC system intensifies, the main EAC jet appears to be strengthening, while the southern extension is becoming more eddying. Using a satellite SST product, in-situ moored observations, and a regional ocean model, we have a shown there is a clear latitudinal gradient in ocean warming on the continental shelf. Shelf waters poleward of where the EAC separates from the coast are warming at at least twice the rate of those equatorward of the separation. This is associated with a strengthening in the main EAC jet upstream of the separation point and an increase in eddy activity downstream of separation. Thus, it would appear that poleward of separation, despite the complex cross-shelf exchange dynamics, the increased advection of warmer EAC water onto the shelf is over-riding local processes such as upwelling and leading to a regional warming trend.

The higher rate of warming which we observe at 34° and 42°, compared to an earlier study by Thompson et al. (2009), points towards an increase in the warming velocity at these sites which is consistent with global ocean warming trends (Cheng et al., 2019). The ability of the EAC-ROMS model to simulate the non-uniform warming of the shelf

waters also lends confidence to the trends being driven by system-scale processes, rather than, for example, small-scale changes in local upwelling winds.

The warming on the shelf in the eddying EAC southern extension is consistent with the increase in poleward penetration of the EAC and its eddies (Cetina-Heredia et al., 2014) and a projected increase in eddy driven poleward heat transport (Oliver et al., 2015) likely driving marine heatwaves in the area (Oliver et al., 2017) . An increase in warm EAC water has already been seen to extend the ocean 'summer' by up to two months at 36°S (Phillips et al., 2020), and is having negative consequences for foraging marine predators such as penguins (Carroll et al., 2016). In a global context, when compared to a global mean warming rate of 0.12°/decade from 1995-2015 (Hausfather et al., 2017), the warming we observe at 27°S is close to the global average, while the shelf warming poleward of separation in the EAC System is more than four times the global average.

Due to the large scale forcing mechanism, we believe that the pattern of non-uniform warming may be common to other coastal regions impacted by western boundary current systems. The shelf temperature trends we observe in the EAC system are consistent with those observed inshore of the Gulf Stream (Shearman & Lentz, 2010). They ascribe the difference in trends up and downstream of separation, as we have in the EAC, to changes in along shelf heat advection, rather than atmospheric changes. Our results support the need for a whole of systems approach to observing and modelling boundary currents along both the length of the system and from the coast to the deep ocean.

Shelf waters and continental margins make up a large part of the primary production and fisheries output in the global ocean (Schmidt et al., 2020). However, most studies on the biological impact of a warming ocean (e.g. Vergés et al. (2014); Ramírez et al. (2017); Free et al. (2019); Jacox et al. (2020)) take trends from datasets too coarse to resolve either shelf trends (Baumann & Doherty, 2013), or extreme events (Pilo et al., 2019). This is especially true in western boundary systems where (cross shelf) spatial scales are small. This has led to the assumption that warming in western boundary current systems is homogeneous, rather than the more nuanced, non-uniform trends shown here. This results in a possible over-estimation of shelf warming trends in some areas and under-estimation in others. As such, spatially resolved studies of warming adjacent to WBCs will enhance our ability to understand the evolution of shelf ecosystems under a warming climate.

References

Archer, M. R., Roughan, M., Keating, S. R., & Schaeffer, A. (2017). On the Variability of the East Australian Current: Jet Structure, Meandering, and Influ-

ence on Shelf Circulation. *Journal of Geophysical Research: Oceans*, *122*(11), 8464–8481. doi: 10.1002/2017JC013097

Baumann, H., & Doherty, O. (2013). Decadal Changes in the World's Coastal Latitudinal Temperature Gradients. *PLoS ONE*, *8*(6), 67596. Retrieved from `www.plosone.org` doi: 10.1371/journal.pone.0067596

Beal, L. M., & Elipot, S. (2016). Broadening not strengthening of the Agulhas Current since the early 1990s. *Nature*, *000*(1). Retrieved from `http://www.nature.com/doifinder/10.1038/nature19853` doi: 10.1038/nature19853

Bowen, M., Markham, J., Sutton, P., Zhang, X., Wu, Q., Shears, N. T., & Fernandez, D. (2017). Interannual variability of sea surface temperature in the southwest Pacific and the role of ocean dynamics. *Journal of Climate*, *30*(18), 7481–7492. doi: 10.1175/JCLI-D-16-0852.1

Bull, C. Y. S., Kiss, A. E., Gupta, A. S., Jourdain, N. C., Argüeso, D., Di Luca, A., & Sérazin, G. (2020). Regional Versus Remote Atmosphere-Ocean Drivers of the Rapid Projected Intensification of the East Australian Current. *Journal of Geophysical Research: Oceans*, *125*(7), 1–18. doi: 10.1029/2019jc015889

Carroll, G., Everett, J. D., Harcourt, R., Slip, D., & Jonsen, I. (2016, 2). High sea surface temperatures driven by a strengthening current reduce foraging success by penguins. *Scientific Reports*, *6*(1), 1–13. Retrieved from `www.nature.com/scientificreports` doi: 10.1038/srep22236

Cetina-Heredia, P., Roughan, M., Liggins, G., Coleman, M. A., & Jeffs, A. (2019). Mesoscale circulation determines broad spatio-temporal settlement patterns of lobster. *PLoS ONE*, *14*(2), 1–20. doi: https://doi.org/10.1371/journal.pone.0211722

Cetina-Heredia, P., Roughan, M., van Sebille, E., & Coleman, M. A. (2014). Long-term trends in the East Australian Current separation latitude and eddy driven transport. *Journal of Geophysical Research: Oceans*, *119*, 4351–4366. doi: 10.1002/2014JC010071

Chen, K., Gawarkiewicz, G. G., Lentz, S. J., & Bane, J. M. (2014). Diagnosing the warming of the Northeastern U.S. Coastal Ocean in 2012: A linkage between the atmospheric jet stream variability and ocean response. *Journal of Geophysical Research: Oceans*, *119*(1), 218–227. doi: 10.1002/2013JC009393

Cheng, L., Abraham, J., Hausfather, Z., & Trenberth, K. E. (2019). How fast are the oceans warming? *Science*, *363*(6423), 128–129. doi: 10.1126/science.aav7619

Colas, F., McWilliams, J. C., Capet, X., & Kurian, J. (2012, 7). Heat balance and eddies in the Peru-Chile current system. *Climate Dynamics*, *39*(1-2), 509–529. doi: 10.1007/s00382-011-1170-6

Deng, X., Griffin, D. A., Ridgway, K., Church, J. A., Featherstone, W. E., White, N. J., & Cahill, M. (2011). Satellite Altimetry for Geodetic, Oceanographic, and Climate Studies in the Australian Region. In *Coastal altimetry* (pp. 473–508). Berlin, Heidelberg: Springer Berlin Heidelberg. Retrieved from `http://link.springer.com/10.1007/978-3-642-12796-0_18` doi: 10.1007/978-3-642-12796-0{_}18

Duran, E., England, M., & Spence, P. (2020). Surface ocean warming around Australia driven by interannual variability and long-term trends in Southern Hemisphere westerlies. *Geophysical Research Letters*, 1–10. doi: 10.1029/2019gl086605

Fiedler, E. K., McLaren, A., Banzon, V., Brasnett, B., Ishizaki, S., Kennedy, J., . . . Donlon, C. (2019). Intercomparison of long-term sea surface temperature analyses using the GHRSST Multi-Product Ensemble (GMPE) system. *Remote Sensing of Environment*, *222*(March 2018), 18–33. Retrieved from `https://doi.org/10.1016/j.rse.2018.12.015` doi: 10.1016/j.rse.2018.12.015

Free, C., Thorson, J., Pinsky, M., Oken, K., Weidenmann, J., & Jensen, O. (2019).

Impacts of historical warming on marine fisheries production. *Science*, *365*(6454). Retrieved from `http://science.sciencemag.org/` doi: 10.1126/science.aax5721

Hausfather, Z., Cowtan, K., Clarke, D. C., Jacobs, P., Richardson, M., & Rohde, R. (2017). Assessing recent warming using instrumentally homogeneous sea surface temperature records. *Science Advances*, *3*(1). Retrieved from `http://advances.sciencemag.org/` doi: 10.1126/sciadv.1601207

Hill, K. L., Rintoul, S. R., Coleman, R., & Ridgway, K. R. (2008). Wind forced low frequency variability of the East Australia Current. *Geophysical Research Letters*, *35*(February), 1–5. doi: 10.1029/2007GL032912

Hu, D., Wu, L., Cai, W., Gupta, A. S., Ganachaud, A., Qiu, B., . . . Kessler, W. S. (2015, 6). *Pacific western boundary currents and their roles in climate* (Vol. 522) (No. 7556). Nature Publishing Group. doi: 10.1038/nature14504

Hu, S., Sprintall, J., Guan, C., McPhaden, M. J., Wang, F., Hu, D., & Cai, W. (2020). Deep-reaching acceleration of global mean ocean circulation over the past two decades. *Science Advances*, *6*(6), 1–9. doi: 10.1126/sciadv.aax7727

Hutchinson, K., Beal, L. M., Penven, P., Ansorge, I., & Hermes, J. (2018). Seasonal Phasing of Agulhas Current Transport Tied to a Baroclinic Adjustment of Near-Field Winds. *Journal of Geophysical Research: Oceans*, *123*(10), 7067–7083. doi: 10.1029/2018JC014319

Imawaki, S., Bower, A. S., Beal, L., & Qiu, B. (2013). *Western Boundary Currents* (No. 1965).

Jacox, M. G., Alexander, M. A., Bograd, S. J., & Scott, J. D. (2020). Thermal displacement by marine heatwaves. *Nature*, *584*(7819), 82–86. Retrieved from `https://doi.org/10.1038/s41586-020-2534-z` doi: 10.1038/s41586-020-2534-z

Kerry, C., Powell, B., Roughan, M., & Oke, P. (2016). Development and evaluation of a high-resolution reanalysis of the East Australian Current region using the Regional Ocean Modelling System (ROMS 3.4) and Incremental Strong-Constraint 4-Dimensional Variational (IS4D-Var) data assimilation. *Geosci. Model Dev*, *9*, 3779–3801. Retrieved from `www.geosci-model-dev.net/9/3779/2016/` doi: 10.5194/gmd-9-3779-2016

Kerry, C., & Roughan, M. (2020a). Downstream Evolution of the East Australian Current System: Mean Flow, Seasonal, and Intra-annual Variability. *Journal of Geophysical Research: Oceans*, *125*(5), 1–28. doi: 10.1029/2019jc015227

Kerry, C., & Roughan, M. (2020b). *A high-resolution, 22-year, free-running, hydrodynamic simulation of the East Australia Current System using the Regional Ocean Modeling System.* UNSW. Retrieved from `https://doi.org/10.26190/5e683944e1369`

Kerry, C., Roughan, M., & Powell, B. (2020). Predicting the submesoscale circulation inshore of the East Australian Current. *Journal of Marine Systems*, *204*(January 2019), 103286. Retrieved from `https://doi.org/10.1016/j.jmarsys.2019.103286` doi: 10.1016/j.jmarsys.2019.103286

Malan, N., Archer, M., Roughan, M., Cetina-heredia, P., Hemming, M., Rocha, C., . . . Queiroz, E. (2020). Eddy-Driven Cross-Shelf Transport in the East Australian Current Separation Zone. *Journal of Geophysical Research : Oceans*, *125*, 1–15. doi: 10.1029/2019JC015613

Messer, L. F., Ostrowski, M., Doblin, M. A., Petrou, K., Baird, M. E., Ingleton, T., . . . Brown, M. V. (2020). Microbial tropicalization driven by a strengthening western ocean boundary current. *Global Change Biology*(April), 1–17. doi: 10.1111/gcb.15257

Oliver, E., Benthuysen, J. A., Bindoff, N. L., Hobday, A. J., Holbrook, N. J., Mundy, C. N., & Perkins-Kirkpatrick, S. E. (2017). The unprecedented 2015/16 Tasman Sea marine heatwave. *Nature Communications*, *8*(May), 1–12. Retrieved from `http://dx.doi.org/10.1038/ncomms16101` doi:

10.1038/ncomms16101

Oliver, E., & Holbrook, N. J. (2014). Extending our understanding of South Pacific gyre "spin-up": Modeling the East Australian Current in a future climate. *Journal of Geophysical Research : Oceans*, *119*, 2788–2805. Retrieved from `http://www.aviso.oceanobs.com` doi: 10.1002/2013JC009591

Oliver, E., O'Kane, T. J., & Holbrook, N. J. (2015, 11). Projected changes to Tasman Sea eddies in a future climate. *Journal of Geophysical Research: Oceans*, *120*(11), 7150–7165. Retrieved from `http://doi.wiley.com/10.1002/2015JC010993` doi: 10.1002/2015JC010993

Phillips, L. R., Carroll, G., Jonsen, I., Harcourt, R., & Roughan, M. (2020). A Water Mass Classification Approach to Tracking Variability in the East Australian Current. *Frontiers in Marine Science*, *7*(June), 1–10. doi: 10.3389/fmars.2020.00365

Pilo, G. S., Holbrook, N. J., Kiss, A. E., & Hogg, A. M. C. (2019). Sensitivity of Marine Heatwave Metrics to Ocean Model Resolution. *Geophysical Research Letters*, *46*(24), 14604–14612. doi: 10.1029/2019GL084928

Qu, T., Fukumori, I., & Fine, R. A. (2019). Spin-Up of the Southern Hemisphere Super Gyre. *Journal of Geophysical Research: Oceans*, *124*(1), 154–170. doi: 10.1029/2018JC014391

Ramírez, F., Afán, I., Davis, L. S., & Chiaradia, A. (2017). Climate impacts on global hot spots of marine biodiversity. *Science Advances*, *3*(2). Retrieved from `http://advances.sciencemag.org/` doi: 10.1126/sciadv.1601198

Rocha, C., Edwards, C. A., Roughan, M., Cetina-Heredia, P., & Kerry, C. (2019). A high-resolution biogeochemical model (ROMS 3.4 + bio_Fennel) of the East Australian Current system. *Geosci. Model Dev*, *12*, 441–456. Retrieved from `https://doi.org/10.5194/gmd-12-441-2019` doi: 10.5194/gmd-12-441-2019

Roughan, M., & Middleton, J. H. (2002). A comparison of observed upwelling mechanisms off the east coast of Australia. *Continental Shelf Research*, *22*(17), 2551–2572. doi: 10.1016/S0278-4343(02)00101-2

Rykova, T., & Oke, P. R. (2015, 11). Recent freshening of the East Australian Current and its eddies. *Geophysical Research Letters*, *42*(21), 9369–9378. Retrieved from `http://doi.wiley.com/10.1002/2015GL066050` doi: 10.1002/2015GL066050

Schaeffer, A., & Roughan, M. (2017). Subsurface intensification of marine heatwaves off southeastern Australia: The role of stratification and local winds. *Geophysical Research Letters*, *44*(10), 5025–5033. doi: 10.1002/2017GL073714

Schaeffer, A., Roughan, M., M Jones, E., & White, D. (2016). Physical and biogeochemical spatial scales of variability in the East Australian Current separation from shelf glider measurements. *Biogeosciences*, *13*(6), 1967–1975. doi: 10.5194/bg-13-1967-2016

Schaeffer, A., Roughan, M., & Morris, B. D. (2013, 5). Cross-Shelf Dynamics in a Western Boundary Current Regime: Implications for Upwelling. *Journal of Physical Oceanography*, *43*(5), 1042–1059. Retrieved from `http://journals.ametsoc.org/doi/abs/10.1175/JPO-D-12-0177.1` doi: 10.1175/JPO-D-12-0177.1

Schilling, H. T., Everett, J. D., Smith, J. A., Stewart, J., Hughes, J. M., Roughan, M., ... Suthers, I. M. (2020). Multiple spawning events promote increased larval dispersal of a predatory fish in a western boundary current. *Fisheries Oceanography*, *29*(4), 309–323. doi: 10.1111/fog.12473

Schmidt, K., Birchill, A. J., Atkinson, A., Brewin, R. J., Clark, J. R., Hickman, A. E., ... Ussher, S. J. (2020). Increasing picocyanobacteria success in shelf waters contributes to long-term food web degradation. *Global Change Biology*, *00*, 1–14. doi: 10.1111/gcb.15161

Shearman, R. K., & Lentz, S. J. (2010). Long-term sea surface temperature variabil-

ity along the U.S. East Coast. *Journal of Physical Oceanography*, *40*(5), 1004–1017. doi: 10.1175/2009JPO4300.1

Shears, N. T., & Bowen, M. M. (2017, 12). Half a century of coastal temperature records reveal complex warming trends in western boundary currents. *Scientific Reports*, *7*(1), 1–9. doi: 10.1038/s41598-017-14944-2

Suthers, I. M., Young, J. W., Baird, M. E., Roughan, M., Everett, J. D., Brassington, G. B., . . . Ridgway, K. (2011). *The strengthening East Australian Current, its eddies and biological effects - an introduction and overview* (Vol. 58) (No. 5). Retrieved from www.elsevier.com/locate/dsr2 doi: 10.1016/j.dsr2.2010.09.029

Tamsitt, V., Talley, L. D., Mazloff, M. R., & Cerovecki, I. (2016, 9). Zonal variations in the Southern Ocean heat budget. *Journal of Climate*, *29*(18), 6563–6579. Retrieved from http://journals.ametsoc.org/jcli/article-pdf/29/18/6563/4071638/jcli-d-15-0630_1.pdf doi: 10.1175/JCLI-D-15-0630.1

Thompson, P. A., Baird, M. E., Ingleton, T., & Doblin, M. A. (2009). Long-term changes in temperate Australian coastal waters: Implications for phytoplankton. *Marine Ecology Progress Series*, *394*, 1–19. doi: 10.3354/meps08297

Vergés, A., Steinberg, P. D., Hay, M. E., Poore, A. G. B., Campbell, A. H., Ballesteros, E., . . . Wilson, S. K. (2014). The tropicalization of temperate marine ecosystems: climate-mediated changes in herbivory and community phase shifts. , *281*(1789), 1–10. doi: 10.1098/rspb.2014.0846

Williams, R. G. (2012). Oceanography: Centennial warming of ocean jets. *Nature Climate Change*, *2*(3), 149–150. doi: 10.1038/nclimate1393

Wu, L., Cai, W., Zhang, L., Nakamura, H., Timmermann, A., Joyce, T., . . . Giese, B. (2012). Enhanced warming over the global subtropical western boundary currents. *Nature Climate Change*, *2*(3), 161–166. Retrieved from http://dx.doi.org/10.1038/nclimate1353\nhttp://www.scopus.com/inward/record.url?eid=2-s2.0-84863254389&partnerID=tZOtx3y1 doi: 10.1038/nclimate1353

Yang, H., Lohmann, G., Krebs-Kanzow, U., Ionita, M., Shi, X., Sidorenko, D., . . . Gowan, E. J. (2020). Poleward Shift of the Major Ocean Gyres Detected in a Warming Climate. *Geophysical Research Letters*, *47*(5). doi: 10.1029/2019GL085868

Yang, H., Lohmann, G., Wei, W., Dima, M., & Liu, J. (2015). Intensification and poleward shift of subtropical western boundary currents under global warming. , *17*, 3734.

Zaba, K., Rudnick, D. L., Cornuelle, B., Gopalakrishnan, G., & Mazloff, M. (2020). Volume and heat budgets in the coastal California Current System: Means, annual cycles and interannual anomalies of 2014-2016. *Journal of Physical Oceanography*(Chereskin 1995), 1435–1453. doi: 10.1175/jpo-d-19-0271.1